Models for Approximating Basilar Membrane Displacement

By J. L. FLANAGAN

(Manuscript received April 1, 1960)

Three analytical models are developed for estimating the displacement of the basilar membrane in the human ear when the sound pressure at the eardrum is known. Frequency-domain data, derived experimentally by Bekesy, are Fourier-transformed to examine the impulse response of the membrane. Time-domain and frequency-domain responses of the models are compared with the experimental data. Excitation of the models by periodic impulses is considered. Calculations of membrane displacement are made for excitation by positive pulses, and by alternately positive and negative pulses. Applicability of the results to the perception of pitch is indicated.

I. INTRODUCTION

In the course of developing an hypothesis to account for results obtained in two experiments on pitch perception,[1,2] it became desirable to have a tractable model from which the displacement of the basilar membrane at a given point could be estimated from a knowledge of the sound pressure at the eardrum. This report describes the results of an effort to deduce such a model.

II. MECHANICAL PROPERTIES OF THE MIDDLE EAR AND COCHLEA

To recall facts and establish a frame of reference, a simplified sketch of the peripheral mechanism of hearing is shown in Fig. 1. The cochlea, actually wound in a snail-shell-like spiral in man, is sketched here unrolled and stretched out. It contains the perilymph fluid and is partitioned longitudinally by a duct formed by Reissner's membrane and the basilar membrane. The duct, roughly triangular in cross section, is filled with another fluid, endolymph. Resting upon the basilar membrane within the cochlea duct is the organ of Corti. This organ, immersed in the endolymph, serves as the termination of the auditory nerve. Bekesy[3] has established that the basilar membrane and Reissner's membrane

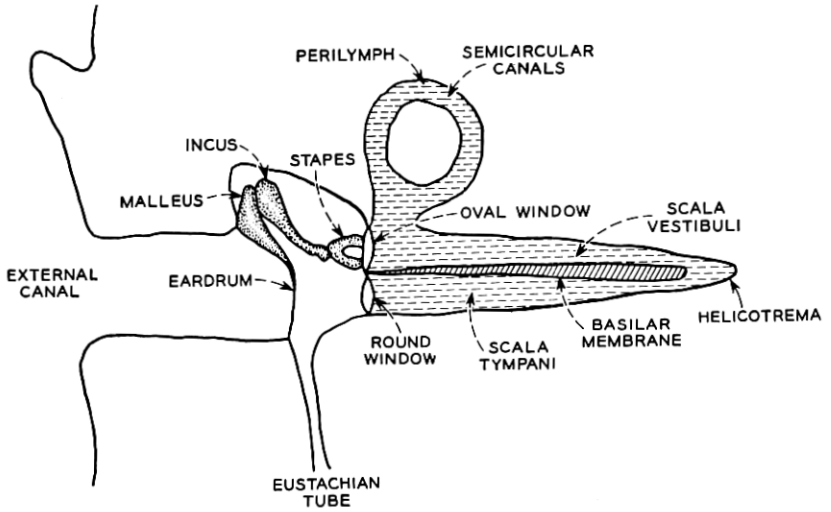

Fig. 1 — Schematic drawing of the human ear.

vibrate cophasically when the ear is stimulated by sound in the lower range of audible frequencies. Because Reissner's membrane does not enter into the present development, only the basilar membrane is sketched in the schematic diagram.

A sound wave impinging on the ear is led down the external canal and sets the drum into vibration. The vibration is transmitted by the ossicular chain to the cochlea, where the piston-action of the stapes foot-plate produces a compressional wave in the fluid. Because of its distributed mass and elastic and viscous constants, and because of the pressure release at the round window, the basilar membrane vibrates selectively according to the frequency content of the stimulus. Displacement of the basilar membrane causes pressure to be exerted (by another membrane in the cochlea duct, the tectorial) upon the hairs emanating from hair cells in the organ of Corti. When the hairs are sufficiently deformed, electrical discharges are produced in the nerve fibers.

The mechanical properties of the cochlea have been studied in detail by Bekesy.[4] He found that, when the stapes is driven sinusoidally with constant amplitude of displacement, the amplitude of displacement of points along the low-frequency (or apical) end of the basilar membrane varies with frequency as shown in Fig. 2. The peak displacement of each point is normalized to unity. His measurements[3] of the difference in phase between the displacement of the stapes and the displacement of

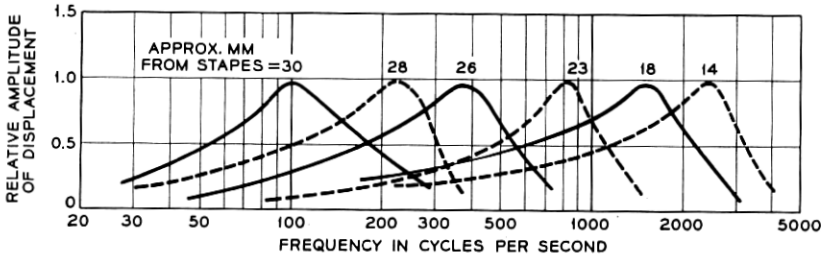

Fig. 2 — Relative amplitude of displacement as a function of frequency for different points along the basilar membrane. The stapes is driven with constant amplitude of displacement (after Bekesy[4]).

points along the membrane are sketched in Fig. 3. In addition to these data, Bekesy found[5] that, when the sound pressure is constant at the eardrum, the magnitude of volume displacement of the round window is nearly constant up to around 2000 cps. To the extent that the perilymph is incompressible and the walls of the cochlea rigid, the volume displacement of the round window is equal that of the stapes footplate.

Data reported by Zwislocki[6] and by Bekesy[5] indicate that, for frequencies below 1000 cps, the over-all impedance of the middle ear and cochlea is predominantly elastic, owing principally to the compliance of

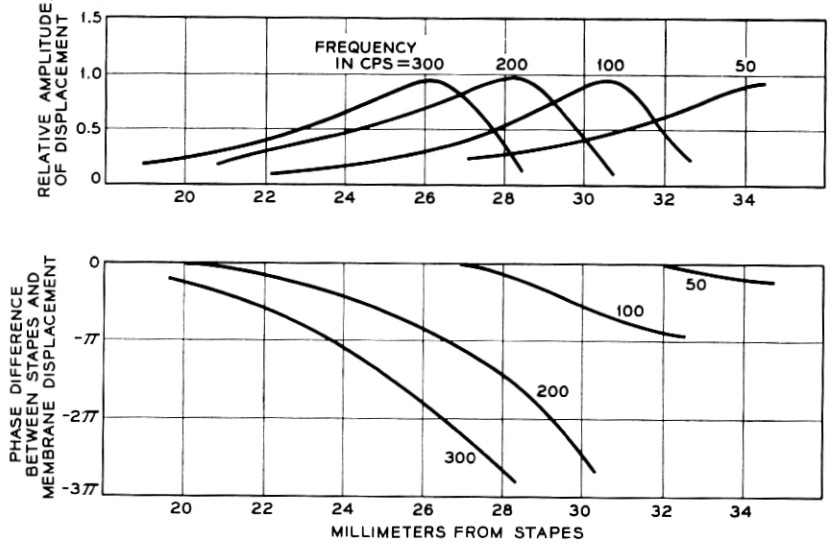

Fig. 3 — Relative amplitude and phase of basilar membrane displacement as a function of distance along the membrane (after Bekesy[3]).

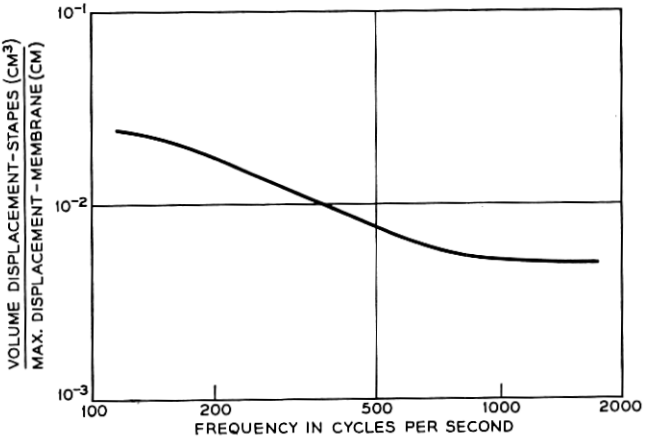

Fig. 4 — Ratio of volume displacement of stapes to peak displacement of basilar membrane (after Bekesy[4]).

the middle ear air cavity, the round window membrane and the ligaments retaining the ossicles and drum. For these frequencies, therefore, the displacement of the stapes is essentially proportional to, and in phase with, the sound pressure at the eardrum. At frequencies above 1000 cps, the inertial and viscous elements of the middle ear and cochlea become more important, and the velocity of the stapes apparently may lag in phase the pressure at the drum by as much as $\pi/2$ radians or more (hence, the stapes displacement may lag the pressure by as much as π radians or more). For frequencies above about 1000 or 2000 cps, the indications are that amplitude of stapes displacement begins to decrease appreciably for constant pressure at the eardrum.*

Because the physical dimensions and mechanical properties of the basilar membrane change along its length (for example, the membrane increases in width, thickness and compliance going toward the apical end), the volume displacement of the membrane per unit length, per unit pressure across it, changes with distance from the stapes. For a constant amplitude of stapes displacement, therefore, the amplitude of the maximally displaced point is not constant with frequency. Bekesy[4] gives the ratio of amplitude of volume displacement of the stapes to amplitude of the maximally displaced point, as shown in Fig. 4. These data show that, for frequencies below 1000 cps, the amplitude of the

* Zwislocki's data suggest a decrease of the order of 12 to 18 db/octave; Bekesy's average data seem to agree roughly with this. In one preparation, however, Bekesy obtained a fall of about 30 db/octave.

maximum increases approximately 4 or 5 db/octave. At around 1000 cps the curve flattens off.

In measurements of the absolute value of membrane displacement, Bekesy finds the maximal displacement at 200 cps to be 10^{-4} cm at the threshold of feeling (about 140 db referred to 0.0002 dyne/cm^2) and, through extrapolation, 10^{-11} cm at the threshold of hearing.* For a given frequency and a given point on the membrane, Bekesy's data indicate that the mechanical vibrations of the stapes and basilar membrane are essentially linearly related until sound pressures above the threshold of feeling are reached. There is evidence, however, that the ear is capable of producing perceptible subjective components at sound levels less than this value.

As stated at the outset, we desire an analytical relation for estimating the basilar membrane displacement at a given point from a knowledge of the sound pressure at the eardrum, valid at least in the frequency range below 1000 cps. It is in this range that the stapes displacement is in phase with, and proportional to, the pressure at the drum. The experimental data that the model must describe are the frequency-domain data just discussed. The approximation problem may, of course, be approached in either the time or frequency domains; usually it is helpful to maintain some insight in both domains. Consequently, we would first like to inquire as to the form of the displacement response of a point toward the low-frequency end of the membrane to an impulse of pressure applied at the eardrum.

III. INVERSE FOURIER TRANSFORMATION OF BEKESY'S DATA

The phase data of Fig. 3 are at best meager, but they are most definitive for the 200-cps point. Let us, therefore, take the 200-cps point for a sample calculation. Deducing the phase response from Fig. 3,† and taking the amplitude response from Fig. 2, we may plot the data as shown in Fig. 5.‡ Let us make two assumptions about the system with which we are dealing: first, the impulse response, $h(t)$, of the point under consideration is Fourier transformable (i.e., $\int_{-\infty}^{\infty} h^2(t)\,dt < \infty$); and second, the system is a stable one having no complex poles with real

* The diameter of a hydrogen atom is about 10^{-8} cm.

† Because peak displacement increases at around 5 db/octave, the possibility exists that the displacement of the point that responds maximally to a given frequency might not be the greatest displacement of the membrane for that frequency. However, the frequency response of a given point generally rises at a rate greater than 5 db/octave in the vicinity of its resonance; consequently, the greatest displacement occurs essentially at the maximally responding point.

‡ As closely as I can determine from the Akustische Zeitschrift data, the maximum displacement of the "200-cps point" falls at about 210–220 cps.

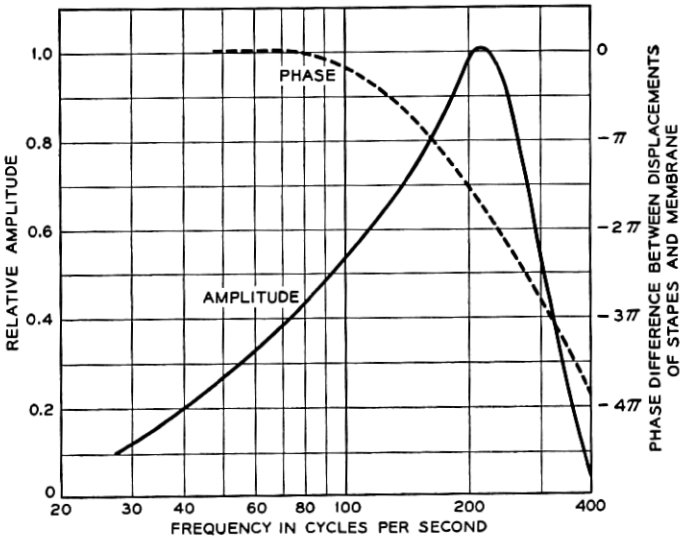

Fig. 5 — Displacement amplitude and phase for a point near the apical end of the basilar membrane. Maximum response occurs for a frequency of about 200 cps. These curves are obtained from data in Figs. 2 and 3.

parts equal to, or greater than, zero (i.e., the system exhibits no output until an input is applied, and the final value of the impulse response is zero).

Taking the data of Fig. 5 as the magnitude, $| H(\omega) |$, and phase, $\Phi(\omega)$, respectively, of the Fourier transform, $H(\omega)$, of the impulse response, $h(t)$, we wish to calculate the inverse transform:

$$h(t) = \frac{1}{2\pi} \int_{-\infty}^{\infty} H(\omega) e^{j\omega t} \, d\omega. \tag{1}$$

In Cartesian form, $H(\omega)$ is

$$H(\omega) = \text{Re } H(\omega) + j \text{ Im } H(\omega),$$

where

$$\begin{aligned} \text{Re } H(\omega) &= | H(\omega) | \cos \Phi(\omega), \\ \text{Im } H(\omega) &= | H(\omega) | \sin \Phi(\omega). \end{aligned} \tag{2}$$

Because Re $H(\omega)$ is an even function of ω and Im $H(\omega)$ an odd function, (1) reduces to:

$$\begin{aligned} h(t) &= \frac{1}{\pi} \int_0^{\infty} \text{Re } H(\omega) \cos \omega t \, d\omega - \frac{1}{\pi} \int_0^{\infty} \text{Im } H(\omega) \sin \omega t \, d\omega \\ &= h_1(t) + h_2(t), \end{aligned} \tag{3}$$

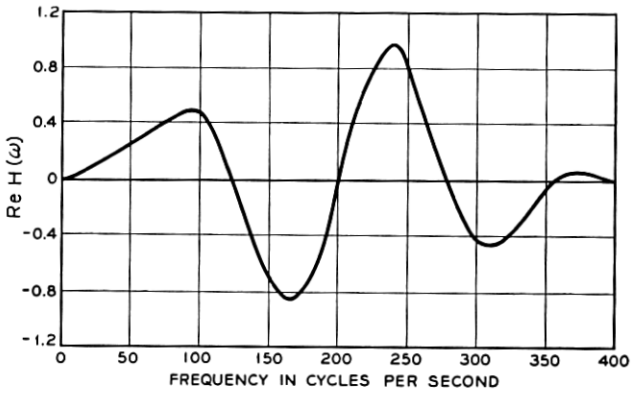

Fig. 6 — Real part of the Fourier transform, $H(\omega)$, whose amplitude and phase spectra are given in Fig. 5.

where $h_1(t)$ is an even function of time and $h_2(t)$ an odd function. Because of the assumptions regarding stability [i.e., $h(t) = 0$, for $t < 0$]:

$$h_1(t) = -h_2(t) \qquad \text{for} \qquad t < 0,$$

and

$$h_1(t) = h_2(t) \qquad \text{for} \qquad t > 0. \tag{4}$$

Hence (3) can be written:

$$h(t) = \frac{2}{\pi} \int_0^\infty \text{Re } H(\omega) \cos \omega t \, d\omega \qquad \text{for} \qquad t > 0. \tag{5}$$

To calculate $h(t)$, then, only Re $H(\omega)$ is needed. For the data of Fig. 5, Re $H(\omega)$ is plotted in Fig. 6.*

In the absence of an analytical specification of Re $H(\omega)$, we have graphically evaluated the integral (5) by using the approximation:

$$h(t_i) = \frac{2}{\pi} \sum_{n=0}^{40} \text{Re } H(\omega_n) \cos \omega_n t_i \Delta\omega, \tag{6}$$

where:

$$\omega_n = n\omega_0,$$

$$\omega_0 = (2\pi)(10) \text{ radians per second}$$

$$\Delta\omega = (2\pi)(10) \text{ radians per second,}$$

$$t_i = (0.4 \times 10^{-3})i, \qquad i = 0, 1, 2, \cdots, 27.$$

* Re $H(\omega)$ was obtained from a large linear plot of $|H(\omega)|$ and $\Phi(\omega)$, not from a semilog plot such as Fig. 5. Estimates, where needed (such as end points of curves), were made on the linear plot.

The impulse response computed by the approximation (6) is shown in Fig. 7.

One notices that the graphical transform yields a nonzero value at $t = 0$, and suggests a nonzero response for $t < 0$. The reason for this might be one of several: (a) the phase and amplitude data of Fig. 5 may not be compatible to satisfy the assumptions made about the system; (b) the data of Fig. 5 suggest that the amplitude response may be band-limited, and it was so treated in the computation; (c) the quantization used in (6) may introduce an error in the calculation of $h(t)$.

Of these three possibilities, the first two seem the more likely sources of discrepancy. The phase data in Fig. 3 suggest that at very low frequencies the phase difference between the displacements of the membrane and stapes is essentially zero. We know, however, that the scalas vestibuli and tympani communicate at the helicotrema. Consequently, a constant displacement of the stapes cannot sustain a constant displacement of the membrane. This argues, therefore, that the amplitude of membrane displacement must go to zero as zero frequency is approached, and the frequency-domain transform of displacement must have at least one zero at the origin of the complex frequency plane. If this is the case, and if the transform is minimum phase, the phase response near zero frequency must be at least $\pi/2$. Intuitively, too, it appears that constant displacement near the helicotrema requires constant velocity of the

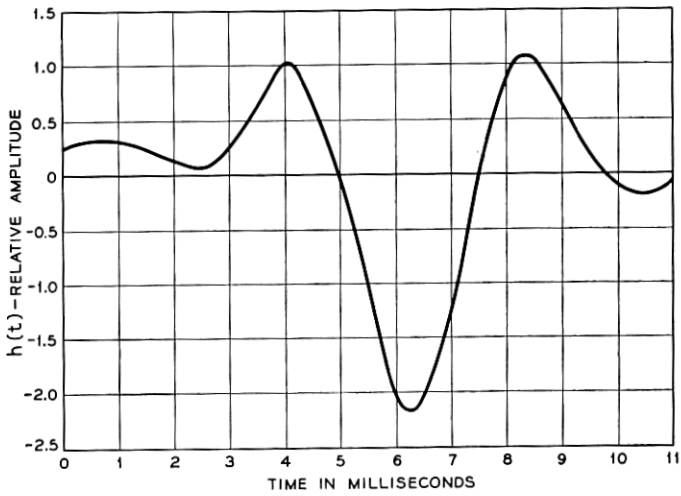

Fig. 7 — Impulse response of the point on the basilar membrane characterized by the amplitude and phase data of Fig. 5. The inverse Fourier transform is obtained by graphical integration of the experimental frequency-domain data.

stapes, arguing again for a derivative relationship between displacements at low frequencies. It seems likely then, that, as low frequencies are approached, the phase of the membrane displacement begins to lead that of the stapes and at zero frequency goes to $\pi/2$. Measurement of the phase relations at low frequencies undoubtedly is difficult, owing to minuscule displacement of the membrane.

In connection with possibility (b), the amplitude data in Fig. 2 suggest that the membrane displacement is essentially band-limited and diminishes to zero for frequencies below about 0.05 and above about 2.0 times the resonant frequency. This should be interpreted, however, with an appreciation of the magnitudes of displacement being observed (on the order of 10^{-4} cm) and the precision attaining thereto. In the graphical transformation, an effort was made to follow the experimental indications as exactly as possible. The amplitude function was treated as mathematically band-limited and was considered to have zero value for frequencies above 400 cps and below 5 cps. This probably is not realistic for the physical system.

Nevertheless, the inverse transform of the experimental data will provide a helpful guide for appraising the responses of the models to be developed in the next section.

IV. MODELS FOR BASILAR MEMBRANE DISPLACEMENT

A model for calculating the displacement of the basilar membrane at a given point must fit the frequency-domain data shown in Figs. 2 and 3. The response curves for various points along the membrane are not unlike those of bandpass filters having relatively sizable in-band delays. The peak values of the curves of Fig. 2 have been normalized to unity, but, as we recall from the previous discussion and from Fig. 4, the peak response rises at about 5 db/octave in the frequency range up to 1000 cps. Above about 2000 cps, the peak response probably falls at something around 12 db/octave, and the stapes displacement is no longer in-phase with the pressure at the drum.

If the data of Figs. 2 and 3 are normalized with respect to the frequency of the maximum response, the curves of Figs. 8 and 9 are obtained, respectively.* Except for the 150-cps case, the phase curves are estimated by reading points vertically from Fig. 3. The 150-cps curve is a single complete phase response published by Bekesy.[3]

* I have replotted these data as carefully as possible from the published curves of Bekesy. In reviewing the literature a small discrepancy appears between the amplitude curves published in Akustische Zeitschrift and those which appear later in the *Handbook of Experimental Psychology*. I judged this to be due to rounding and smoothing in redrafting the latter, and hence gave more weight to the earlier data.

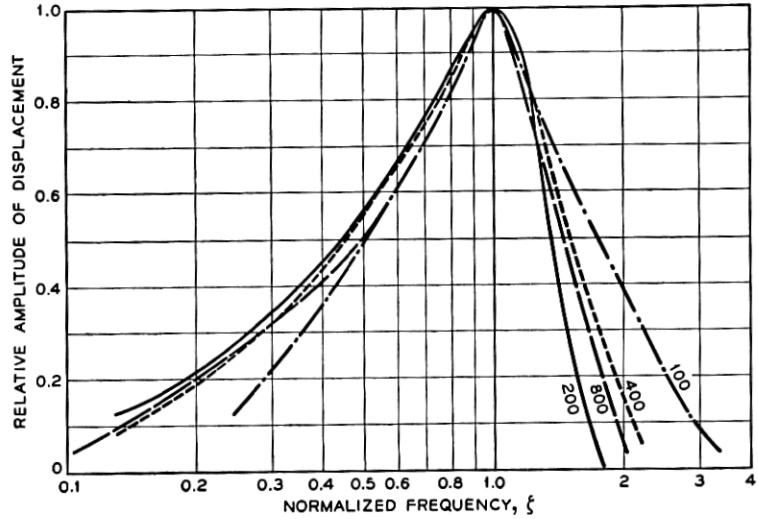

Fig. 8 — The experimental displacement data of Fig. 2 plotted with frequency normalized in respect to the frequency of maximum displacement.

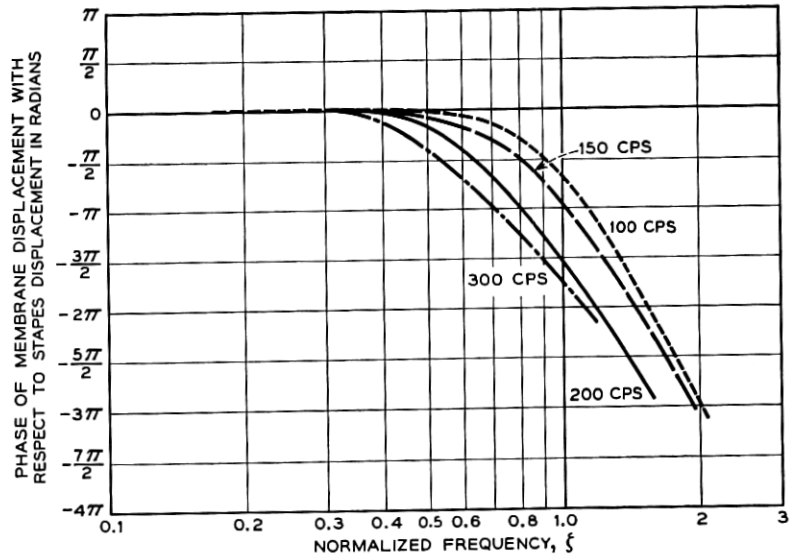

Fig. 9 — Phase responses deduced from data in Fig. 3. Frequency is normalized as in Fig. 8.

One notices that, except for the 100-cps case, the amplitude curves fall close together and represent resonances whose bandwidths are essentially constant percentages of the resonant frequencies (i.e., constant "Q"). The 100-cps curve is slightly broader than the others. The lower skirt of the amplitude curves rises at about 6 db/octave, while the upper skirt falls at approximately 20 to 30 db/octave. The total phase change in passing through a resonance is of the order of 3π. The phase curves for the lower frequency points have the greater slopes (i.e., $d\Phi/d\omega$) inside the passbands, and the delay for the lower frequency points is therefore greater. (This is, of course, as it should be, since the time required to propagate energy from the eardrum to points near the apical end of the membrane is greater than it is for points lying at the basal end.)

As a minor digression, it is interesting to notice that the slopes of the phase curves in the vicinity of resonance indicate delay values about twice as large as the transit times measured by Bekesy.[4] Measuring the slopes of the phase curves in this region (again, from the linear plot) yields:

Resonant Frequency, f	Phase Delay, $d\phi/d\omega$	$2\pi f(d\phi/d\omega)$
100 cps	11.8 msec	7.4 radians
150	7.2	6.8
200	6.4	8.0
300	4.5	8.5

These times represent the delays of the frequency components containing the greatest portion of the stimulus energy, and do not represent the times at which a response first appears (i.e., transit times). Looking back at the graphically determined impulse response for the 200-cps point (Fig. 7), one sees that the greatest displacement occurs at approximately 6.3 milliseconds. The time at which the response essentially begins is of the order of 2.5 milliseconds, which is in close agreement with Bekesy's measurements. It is also interesting to note in passing that the product of resonant frequency and delay near resonance (i.e., the third column) is roughly constant. This fact will be utilized in adjusting the phase response of the models.

To return to the question of fitting a function to the frequency-domain data, at least for the frequency range below 1000 cps, let us consider a model whose Laplace transform is the ratio of rational polynomials. There will be, of course, an infinite number of possibilities for fitting the data, depending upon the criterion and precision of fit. We would, however, like to have an approximation that is both computationally simple and hopefully adequate to explain certain subjective results in pitch-matching. Any criterion of fit must ultimately have its roots in psychoacoustic phenomena. Since such cannot be specified at this time, it would

seem that conventional curve-fitting techniques and least-squares criteria might be discarded in favor of a basically intuitive approach.

The skirt slopes of the amplitude curves suggest a frequency function that has a simple zero in the vicinity of the origin of the complex frequency plane, and a denominator whose degree is about four or five greater than that of the numerator. The relationship between the real and imaginary parts of its complex conjugate poles ought to be such as to maintain the constant-percentage bandwidth character of the responses. The amplitude at resonance ought to vary in the manner prescribed earlier, and the phase and delay characteristics presumably should be representative of the experimental data. (The question of phase at low frequencies will necessarily receive some further consideration.)

As one of the simpler possibilities for approximating the amplitude and phase data, consider a function having two pairs of synchronously tuned complex-conjugate poles, one negative-real axis pole, and one negative-real axis zero near the origin. Adorned with necessary constants, such a function has a Laplace transform:

$$F_1(s) = c_1\beta^{4+r}\left(\frac{s+\epsilon}{s+\gamma}\right)\left[\frac{1}{(s+\alpha)^2+\beta^2}\right]^2 e^{-sT}, \tag{7}$$

where:

c_1 is a positive real scale factor which yields the appropriate absolute value of displacement;

β^{4+r} is a factor that produces the proper variation in amplitude of resonance with resonant frequency (if, as previously suggested, a figure of 5 db/octave rise in the resonant peak is accepted, then $r = 0.83$);

e^{-sT} is a delay factor (T seconds) to bring the phase response into line with the experimental phase data.

The function has second-order poles at $s = -\alpha \pm j\beta$, a simple pole at $s = -\gamma$ and a simple zero at $s = -\epsilon$. By virtue of the constant-percentage bandwidth properties of the membrane resonances, we let β and α be related by a constant: $\beta = k\alpha$. The value of the function for real frequencies (i.e., $s = j\omega$) is:

$$F_1(j\omega) = c_1\beta^{4+r}\left(\frac{\epsilon+j\omega}{\gamma+j\omega}\right)\left[\frac{1}{\left(\beta^2+\frac{\beta^2}{k^2}-\omega^2\right)+j\frac{2\beta}{k}\omega}\right]^2 e^{-j\omega T}. \tag{8}$$

As with the experimental data, it is convenient to work with frequency normalized. Let $\zeta = (\omega/\beta)$.* Then (8) becomes:

$$F_1(j\zeta) = c_1\beta^r \left(\frac{\frac{\epsilon}{\beta} + j\zeta}{\frac{\gamma}{\beta} + j\zeta}\right)\left[\frac{1}{\left(1 + \frac{1}{k^2} - \zeta^2\right) + j\frac{2}{k}\zeta}\right]^2 e^{-j\zeta\beta T}. \quad (9)$$

One notices that fitting the phase and amplitude data of Bekesy near to zero frequency presents somewhat of a dilemma (as it does with all other minimum-phase functions that we have considered). To diminish the amplitude response at low frequencies, one needs the zero of the function close to the origin. Although the phase at zero frequency obviously remains zero so long as the function zero is in the left-half plane, the phase "bulges" appreciably positive at low frequencies if the zero is placed too close to the origin. By empirical adjustment of the parameters, a compromise position was obtained for the zero, and corresponding values for k, T and γ were deduced. The values arrived at are:

$$\begin{aligned} \frac{\epsilon}{\beta} &= 0.1, & k &= 2.0, \\ \frac{\gamma}{\beta} &= 1.0, & T &= \frac{3\pi}{4\beta} \text{ seconds.} \end{aligned} \quad (10)$$

In order to match phase responses, one notices that the delay, T, is taken to vary inversely with the resonant frequency, β. For the constant chosen, the added delay at 100 cps, for example, is approximately 4 milliseconds. This delay, in conjunction with the ω-dependent delay, is in reasonable agreement with Bekesy's measurements of transit time down the membrane.

A plot of

$$\frac{|F_1(j\zeta)|}{|F_1(j\zeta_{\max})|},$$

where $\zeta_{\max}$ is the frequency of peak displacement, is given in Fig. 10.† The hatched region represents, for comparison, the variability among the

* This normalizes real frequency with respect to the imaginary part of the pole frequency. The latter is not necessarily the same as the frequency of maximum response.

† Note that for the present parameters the resonant peak does not fall exactly at $\zeta = 1.0$, but more nearly at $\zeta = 0.95$.

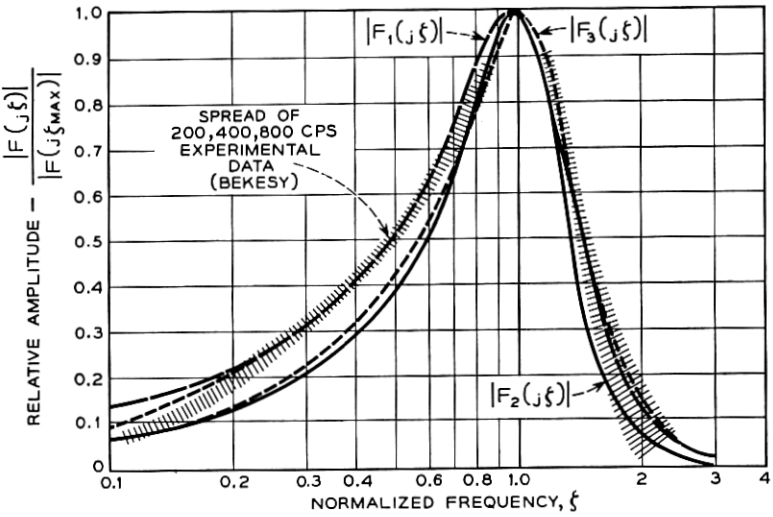

Fig. 10 — Frequency responses of the models compared with experimental data.

200, 400 and 800 cps curves of Fig. 8. A plot of $\angle F_1(j\zeta) = \Phi_1(j\zeta)$ is given in Fig. 11.

If the experimental phase data at low frequencies are not taken too seriously, and the phase of (9) allowed to approach $\pi/2$, then the zero might be placed at the origin (i.e., $\epsilon = 0$). The amplitude response for this situation is shown by the dashed portion of the $|F_1(j\zeta)|$ curve in Fig. 10.

At high frequencies, function (9) attenuates as ζ^{-4}, or at about 24 db/octave. Some of Bekesy's data indicate attenuations slightly greater than this. As another possibility, therefore, a function having a simple zero at the origin and third-order, complex-conjugate poles was considered. Its Laplace transform is:

$$F_2(s) = c_2\beta^{5+r}\frac{s}{[(s+\alpha)^2+\beta^2]^3}e^{-sT}, \tag{11}$$

where the constants are defined in a manner similar to (7). The real frequency response in terms of normalized frequency is:

$$F_2(j\zeta) = c_2\beta^r\frac{j\zeta}{\left[\left(1+\frac{1}{k^2}-\zeta^2\right)+j\frac{2}{k}\zeta\right]^3}e^{-j\zeta\beta T}. \tag{12}$$

A reasonable fit to the resonant bandwidth is obtained for $k = 2.0$ with

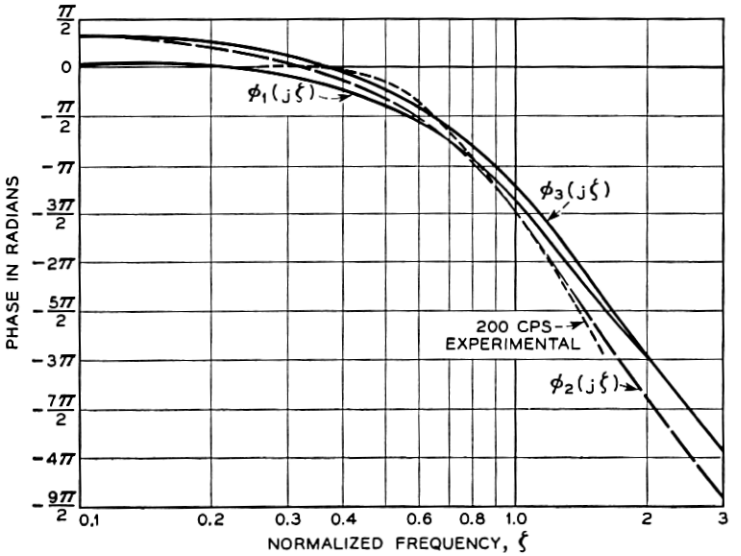

Fig. 11 — Phase responses of the models.

$\beta T = 3\pi/4$, as before. For these values, a plot of $|F_2(j\zeta)|/|F_2(j\zeta_{max})|$ is given in Fig. 10 and $\angle F_2(j\zeta)$ is given in Fig. 11.

With a thought toward inverse transformations for the approximating functions, one function that provides a respectable fit and has a particularly simple inverse transform is the following:

$$F_3(s) = c_3\beta^{4+r}\frac{s^2 + 2\alpha s + \left(\alpha^2 - \frac{\beta^2}{3}\right)}{[(s+\alpha)^2 + \beta^2]^3}e^{-sT}. \tag{13}$$

Or, in terms of the normalized real frequency,

$$F_3(j\zeta) = c_3\beta^r\frac{\left(\frac{1}{k^2} - \frac{1}{3} - \zeta^2\right) + j\frac{2}{k}\zeta}{\left[\left(\frac{1}{k^2} + 1 - \zeta^2\right) + j\frac{2}{k}\zeta\right]^3}e^{-j\zeta\beta T}. \tag{14}$$

This function has simple zeros at $s = \alpha(-1 \pm k/\sqrt{3})$ and third-order poles at $s = \alpha(-1 \pm jk)$. The function obviously becomes nonminimum phase for $k > \sqrt{3}$. Because the separation between zeros is $2k/\sqrt{3}$, the zero at $s = \alpha(-1 + k/\sqrt{3})$ has the greatest influence on amplitude response for the minimum phase conditions (i.e., $k \gtrless \sqrt{3}$). For values of $k = 1.7$ and $\beta T = 3\pi/4$, the amplitude and phase responses of (14) are shown in Figs. 10 and 11, respectively.

V. INVERSE TRANSFORMS OF THE MODELS

It is pertinent to examine the inverse transforms of the models (7), (11) and (13) (i.e., their responses to unit impulses applied at $t = 0$) and to compare these responses with the impulse response obtained for the experimental data (Fig. 7).

Inverse transforming (7) is a particularly cumbersome procedure. In the interest of conciseness, the details of the inverse transformations for all the functions are relegated to the Appendix. Only the results will be used here. For function $F_1(s)$, the impulse response turns out to be:

$$\begin{aligned} f_1(t) &= c_1\beta^{1+r}\{[0.033 + 0.360\beta(t - T)]e^{-\beta(t-T)/2}\sin\beta(t - T) \\ &\quad + [0.575 - 0.320\beta(t - T)]e^{-\beta(t-T)/2}\cos\beta(t - T) \\ &\quad - 0.575\, e^{-\beta(t-T)}\} \qquad \text{for} \quad t \geqq T \\ f_1(t) &= 0 \qquad\qquad\qquad\qquad\quad \text{for} \quad t < T, \end{aligned} \tag{15}$$

where T is the previously specified delay.

In a similar manner, the inverse transform of $F_2(s)$ is:

$$\begin{aligned} f_2(t) &= \\ &\frac{c_2\beta^{1+r}}{8}\left[\left\{\frac{[\beta(t - T)]^2}{2} + \beta(t - T) - \tfrac{3}{2}\right\}e^{-\beta(t-T)/2}\sin\beta(t - T)\right. \\ &\quad \left. + \{-[\beta(t - T)]^2 + \tfrac{3}{2}\beta(t - T)\}e^{-\beta(t-T)/2}\cos\beta(t - T)\right] \\ &\qquad\qquad\qquad\qquad\qquad\qquad \text{for} \quad t \geqq T, \\ f_2(t) &= 0 \qquad\qquad\qquad\qquad\qquad\quad \text{for} \quad t < T. \end{aligned} \tag{16}$$

As indicated earlier, the inverse transform of $F_3(s)$ is particularly simple, this being the principal reason for presenting its fit. Its inverse is:

$$\begin{aligned} f_3(t) &= \frac{c_3\beta^{1+r}}{6}[\beta(t - T)]^2 e^{-\beta(t-T)/1.7}\sin\beta(t - T) \qquad \text{for} \quad t \geqq T \\ f_3(t) &= 0 \qquad\qquad\qquad\qquad\qquad\qquad\qquad\quad \text{for} \quad t < T. \end{aligned} \tag{17}$$

For comparison purposes, the impulse responses $f_1(t)$, $f_2(t)$ and $f_3(t)$ are plotted in Fig. 12, together with the graphically determined response of Fig. 7. In this plot relative delays have been equalized to compare waveforms. Because the scale constants c_1, c_2 and c_3 have not been taken into account, the amplitude scales for the different curves are relative. The curves have been plotted, however, for approximately equal

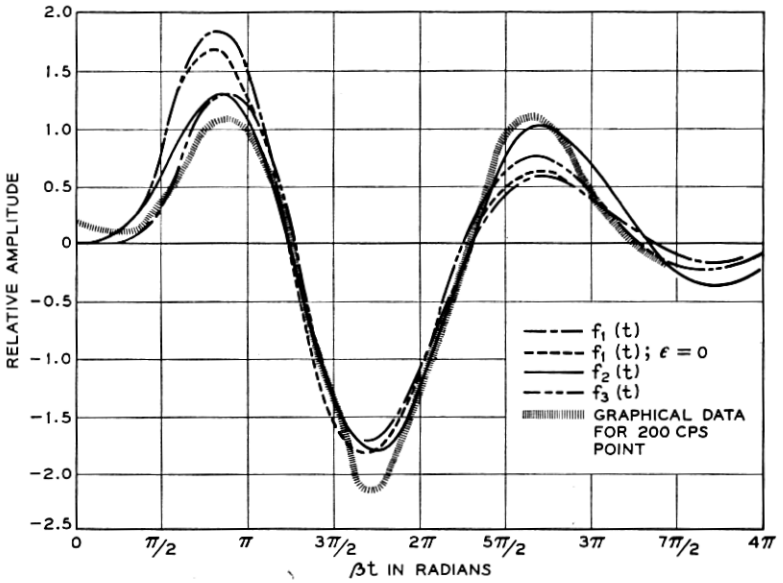

Fig. 12 — Impulse responses of the models. These displacement functions are the inverse transforms of the frequency-domain data in Figs. 10 and 11. Time delay has been equalized to compare waveforms. Locations of absolute origins are given in the text.

peak-to-peak values. The fits to the experimental data do not seem unrealistic, in view of the questions raised earlier. One notices that, in most instances, the positive impulses produce the greatest deflection in the negative direction. Equalization of the delays to bring the curves into coincidence were such as to make the absolute origins ($\beta t = 0$) for each response the following number of radians to the left:

Function	Radians to Absolute Origins
200 cps, experimental	2.3
$f_1(t)$	1.9
$f_2(t)$	2.4
$f_3(t)$	1.5

Of the functions displayed, $f_2(t)$ and $f_3(t)$ appear to fit the graphically derived impulse response better than $f_1(t)$ does. In the frequency domain, however, $F_1(s)$ appears to afford the slightly better fit.

VI. RESPONSE OF MODELS TO PERIODIC IMPULSE EXCITATION

If an excitation of periodic unit impulses is delivered to a linear system, the periodic response is a doubly infinite, linear superposition of

responses to single impulses, or:

$$g(t) = \sum_{n=-\infty}^{\infty} f(t - n\tau), \tag{18}$$

where $f(t)$ is the response to a single impulse, applied at $t = 0$, τ is the period of excitation and $g(t)$ is the periodic response. If $F(\omega)$ is the Fourier transform of $f(t)$, it can be shown that:

$$g(t) = \sum_{n=-\infty}^{\infty} \frac{1}{\tau} F(n\omega_0) e^{jn\omega_0 t}, \tag{19}$$

where $\omega_0 = 2\pi/\tau$ is the fundamental frequency of excitation. Because $g(t)$ is a real function of time for a physically realizable system, the amplitude spectrum is even; i.e., $| F(\omega) | = | F(-\omega) |$; and the phase spectrum is odd; i.e., $\Phi(\omega) = -\Phi(-\omega)$. Relation (19) can therefore be written:

$$g(t) = \frac{\omega_0}{2\pi}\left\{| F(0) | + 2 \sum_{n=1}^{\infty} | F(n\omega_0) | \cos [n\omega_0 t + \Phi(n\omega_0)]\right\}. \tag{20}$$

By way of example, let us look at the response of function $F_1(\omega)$ [see (8)] to an excitation of periodic impulses. Suppose we first take the case where $F_1(\omega)$ specifies a point on the membrane tuned to the fundamental frequency of excitation. Let the resonant frequency of the point be $\beta_x = \omega_0$. Then $\zeta = \omega/\omega_0 = n\omega_0/\omega_0 = n$ and $F_1(n\omega_0) = F_1(\zeta = n)$, and the periodic response is:

$$g_x(t) = \frac{\beta_x}{2\pi}\left\{F_1(\zeta = 0) + 2 \sum_{n=1}^{\infty} | F_1(\zeta = n) | \cos [n\beta_x t + \Phi_1(\zeta = n)]\right\}. \tag{21}$$

As determined in previous calculations, values of $F_1(\zeta)$ are:

n	ζ	$\left\lvert \frac{F_1(\zeta)}{c_1 \beta_x{}^2} \right\rvert$	$\phi(\zeta)$, degrees
0	0	0.06	0
1	1	0.67	−248
2	2	0.08	−534
3	3	0.01	−706

Obviously, in this case the displacement response of the membrane is principally fundamental, the second harmonic being slightly more than one-tenth the amplitude of the fundamental. A plot, on a relative amplitude scale, of these first four terms is shown in Fig. 13(a).

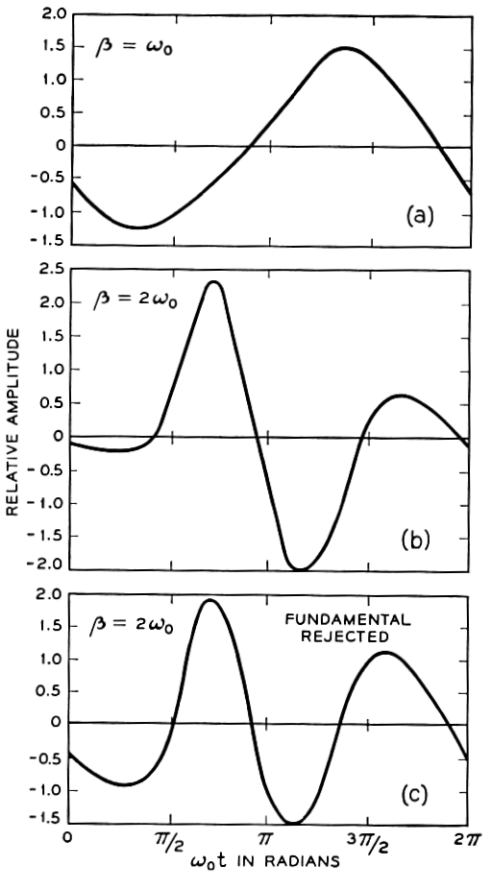

Fig. 13 — Displacement responses of model $F_1(s)$ to excitation by periodic impulses. The three conditions represent: (a) the displacement of a point on the membrane resonant to the fundamental frequency, ω_0 ; (b) the displacement of a point resonant to the second harmonic; (c) the same as (b) except with the fundamental frequency component eliminated from the stimulus.

Consider next a point on the membrane tuned to the second harmonic of the stimulus (i.e., $\beta_y = 2\omega_0 = 2\beta_x$). Then $\zeta = \omega/2\omega_0 = n\omega_0/2\omega_0 = n/2$ and $F_1(n\omega_0) = F_1(\zeta = n/2)$. In this case:

$$g_y(t) = \frac{\beta_y}{4\pi}\left\{F_1(\zeta = 0) + 2\sum_{n=1}^{\infty}\left|F_1\left(\zeta = \frac{n}{2}\right)\right|\cos\left[n\frac{\beta_y}{2}t + \Phi_1\left(\zeta = \frac{n}{2}\right)\right]\right\}. \tag{22}$$

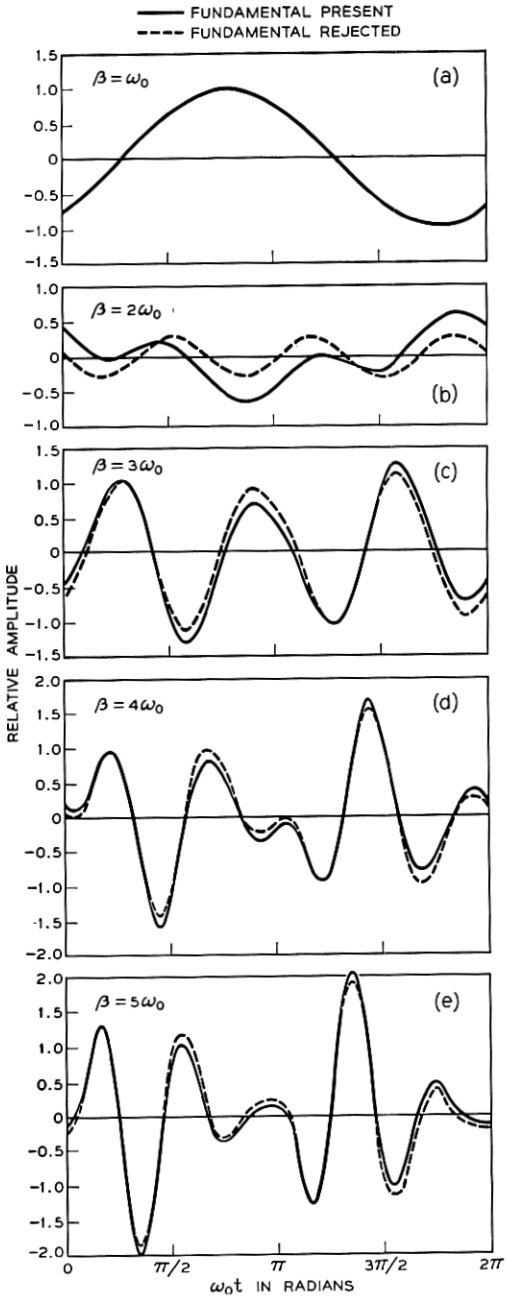

Fig. 14 — Displacement responses of model $F_2(s)$ to periodic excitation by alternate positive and negative impulses. The five conditions represent the displacements of membrane points respectively resonant to: (a) fundamental frequency; (b) second harmonic; (c) third harmonic; (d) fourth harmonic and (e) fifth harmonic. The dashed curves are the displacements when the fundamental component is eliminated from the stimulus.

Functional values for this case from previous computations are:

n	ζ	$\left\lvert \frac{F_1(\zeta)}{c_1 \beta_y{}^r} \right\rvert$	$\phi(\zeta)$, degrees
0	0	0.06	0
1	0.5	0.37	−69
2	1.0	0.67	−248
3	1.5	0.27	−422
4	2.0	0.08	−534
5	2.5	0.03	−626

Because of the form of (9), note that the amplitude scale factors for $g_y(t)$ and $g_x(t)$ are in the ratio $(\beta_y/\beta_x)^r = 2^r$.* The response $g_y(t)$ of the point resonant at the second harmonic of the excitation is plotted in Fig. 13(b).

If the stimulus is ideally high-pass filtered to remove the dc and fundamental terms, then the periodic response at point β_y is that shown in Fig. 13(c).

The shape of a single period at β_y, with the fundamental present, is already similar to the impulse response. If one examines points tuned higher in frequency, the time resolution increases because the bandwidth increases, and the response becomes more and more identifiable as repeated impulse responses (i.e., nonoverlapping impulse responses).

An even more instructive insight is obtained if one considers periodic excitation by alternately positive and negative impulses. Such a train is odd-harmonic in equal amplitude† and, like the repeated positive pulses, has a phase spectrum that is zero. To vary the example, let us consider the response of $F_2(s)$ [see (11)] to this excitation. Following an approach identical to that just described, but dealing only with odd spectral components, the responses of Fig. 14 are obtained. Once again we recall that the amplitude scales, shown here as relative, are in the ratio β^r.

The response of a point tuned to the fundamental is essentially a sinusoid at the fundamental frequency and is shown in Fig. 14(a). The displacement of the membrane point tuned to the second harmonic (where there is no stimulus energy) is shown in Fig. 14(b). It exhibits a displacement in which the fundamental periodicity can be discerned when the fundamental component is present. Without the fundamental the response is relatively low-amplitude third harmonic. The point tuned to the third harmonic, Fig. 14(c), displaces essentially at the third har-

* The implication here, of course, is that we are still dealing with frequency ranges below 1000 cps, where the membrane resonances are assumed to vary in peak displacement, as previously discussed.

† The equal-amplitude spectral lines have twice the amplitude of those for repeated positive impulses.

monic frequency whether the fundamental is present or absent. The point tuned to the fourth harmonic, Fig. 14(d), begins to exhibit fundamental periodicity again, regardless of whether fundamental is present or not. The point tuned to the fifth harmonic, Fig. 14(e), yields a response which is very nearly nonoverlapping, superposed impulse responses.

Quantification of the membrane displacement in this manner offers a basis for a number of useful speculations on the perception of periodic pulses.

VII. CONCERNING RELATIVE AMPLITUDES OF DISPLACEMENT

Since relative amplitude of displacement may be of importance in the conversion of membrane displacement into nervous activity, it is worthwhile to examine amplitude relations further. We have seen that, if the membrane is excited with periodic impulses at a fundamental frequency to which a point near the apical (low-frequency) end is resonant, this point executes a displacement which is nearly the fundamental sinusoid. A point toward the basal (high-frequency) end, whose resonance curve embraces a substantial number of harmonics, yields a periodic response, which is essentially a succession of negligibly-overlapping impulse responses. Because such points respond simultaneously (except for transit delay), and because their peak amplitudes have implications in hypotheses about pitch perception, let us compare the peak amplitudes of a "fundamental-responding" point with that of an "impulse-responding" point. For the sake of varying the examples further, let us work with model $F_3(s)$, in (13), and its impulse response $f_3(t)$, in (17). We are interested in the absolute extremum of (17). The times of the extrema can be found by differentiating (17), setting to zero and solving, which gives:

$$t_{\max} = \frac{1}{\beta} \tan^{-1}\left[\frac{1.7\beta(t - T)}{\beta(t - T) - 3.4}\right], \qquad t > T. \tag{23}$$

The envelope maximum occurs at:

$$t_{\max \text{ envel}} = \left(\frac{3.4}{\beta} + T\right). \tag{24}$$

It is not necessary to solve the trancendental relation (23), since we already have (17) plotted to a reasonable precision in Fig. 12. Using the latter data, we get for the absolute maximum of $f_3(t)$,

$$|f_3(t)|_{\max} = \frac{c_3\beta_p^{1+r}}{6}(1.4) = (0.23)c_3\beta_p^{1+r}, \tag{25}$$

where the subscript p denotes a point toward the high-frequency end of the membrane. In a parallel manner, the amplitude of a point, q, tuned to the fundamental frequency can be obtained from relation (20). In this case, $\beta_q = \omega_0$ and

$$\begin{aligned} |\, g_3(t)\,|_{\text{fund}} &\cong \frac{\omega_0}{2\pi} 2\,|\, F_3(\zeta = 1)\,| \\ &\cong \frac{\omega_0}{\pi} c_3 \beta_q{}^r (0.83) \\ &\cong c_3 \beta_q{}^{1+r} (0.26). \end{aligned} \tag{26}$$

The ratio of these two peak displacements is, therefore

$$R_3 = \frac{|\, f_3(t)\,|_{\max}}{|\, g_3(t)\,|_{\text{fund}}} = (0.88)\left(\frac{\beta_p}{\beta_q}\right)^{1+r}. \tag{27}$$

If the same computations are made for the other two models, $F_1(s)$ and $F_2(s)$, the ratios are:

$$\begin{aligned} R_1 &= (0.80)\left(\frac{\beta_p}{\beta_q}\right)^{1+r}, \\ R_2 &= (0.82)\left(\frac{\beta_p}{\beta_q}\right)^{1+r}. \end{aligned} \tag{28}$$

Since $\beta_p > \beta_q$ and since the experimentally determined exponent $r \approx 0.8$, the peak amplitudes of the impulse-responding points exceed those of the fundamental-responding points, at least in the frequency range below 1000 cps (i.e., roughly over the apical half of the membrane).

VIII. EVALUATION OF SCALE CONSTANTS c_1, c_2 AND c_3

Bekesy's data show that the maximum deflection of the basilar membrane at a frequency of 1000 cps and a sound pressure level of 134 db referred to 0.0002 dyne/cm^2 (i.e., 10^3 dynes/cm^2) is approximately 10^{-4} cm. His measurements also indicate that the mechanical functioning of the middle and inner ear is essentially linear to the threshold of feeling. In the models, therefore, the constants c_1, c_2 and c_3 should be chosen to provide peak displacements at resonance equal to

$$(10^{-7}\ \text{cm}^3/\text{dyne})\left[\frac{\beta}{2\pi(1000)}\right]^r.$$

The amplitude responses of the models at resonance are:

$$\begin{aligned} |F_1(\zeta = 1.0)| &= c_1\beta^r(0.66), \\ |F_2(\zeta = 1.0)| &= c_2\beta^r(0.92), \\ |F_3(\zeta = 1.0)| &= c_3\beta^r(0.83). \end{aligned} \tag{29}$$

The values of the constants, therefore, should be:

$$\begin{aligned} c_1 &= \frac{10^{-7}}{(0.66)[2\pi(1000)]^r}, \\ c_2 &= \frac{10^{-7}}{(0.92)[2\pi(1000)]^r}, \\ c_3 &= \frac{10^{-7}}{(0.83)[2\pi(1000)]^r}. \end{aligned} \tag{30}$$

IX. APPLICATION TO PITCH PERCEPTION

As suggested at the outset, the present computations were precipitated by a particular need. In drafting a paper to report two earlier experiments on pitch perception,[1,2] it became painfully obvious, as soon as the discussion section was reached, that little quantitative basis existed for interpreting the subjective data. The models described here were developed in an attempt to alleviate this situation.

In the pitch experiments it became necessary to explain how three different modes of pitch perception arise when periodic pulse trains stimulate the ear. One mode ascribes a pitch to the stimulus equal to the pulse rate, regardless of the polarity pattern of the train; in other words, positive pulses (condensations) are not discriminated from negative pulses (rarefactions). A second mode ascribes a pitch equal to the mathematical fundamental whether energy is present at this frequency; this mode includes the situation which has been labeled "residue" phenomenon. The third mode assigns a pitch equal to the frequency of the lowest spectral component present in the stimulus.

The first mode characteristically operates at low values of pulse rate (usually below 100 pps in unmasked situations). The second usually obtains for fundamental frequencies in the approximate range 200 to 500 cps. The third seems to hold for fundamental frequencies around 1000 cps and higher when the lowest-frequency component is rejected by HP filtering.

Without launching into the details of the psychophysical experiments, the applicability of the models to the perception of pulses can at least

be indicated. It is of consequence, for example, to ascertain to what extent the subjective pitch modes are manifested in the mechanical operation of the cochlea. Looking again at Fig. 14, one can observe displacement patterns that might be considered favorable for giving rise to the pitch modes just outlined. This presumes, of course, certain hypotheses about the mechanism of converting displacement information into electrical discharges in the nerve fiber. A discussion of these important details, however, is more appropriate in another place. Even so, Fig. 14 suggests several things.

When the membrane is excited over most of its length by a periodic pulse stimulus, the higher-frequency portion probably is effective in supplying only pulse-rate information, no matter what the polarity pattern of the train. In this region of the membrane the pulses are well resolved in time (i.e., the displacement is essentially nonoverlapping impulse responses), and the "overshoot" of the response to each pulse is substantial. Under certain assumptions about the transduction of displacement into nervous activity, the latter fact can be construed as favorable for eliciting nerve volleys in synchrony with each pulse.*

Information on fundamental frequency might be manifested in two ways: (a) If the fundamental component is present in the stimulus, then the point on the membrane tuned to the fundamental responds strongly with near sinusoidal displacement. (b) If, on the other hand, the fundamental is absent, the lowest-frequency part of the membrane receiving excitation will embrace a small number of spectral lines within its frequency response. Its displacement generally will exhibit the fundamental periodicity in a form favorable for triggering one nerve volley per fundamental period.

So far these comments have not considered the importance of relative amplitudes of displacement. This question appears to be of particular consequence in evoking the second, or fundamental, pitch mode. Although the indications are that most significant neural information originates from the point of greatest displacement, there is evidence that subjects may give preference to the fundamental mode over the pulse-rate mode even though the former may be correlated with smaller membrane displacements than is the latter. Relative amplitudes of displacement very likely undergo nonsimple transformations in the neural conversion process.

Still open, too, is the question of the third pitch mode. Although our models are limited to the frequency range below 1000 cps (because they

* There also is evidence that the transduction may be sensitive to spatial derivatives of displacement as well as to displacement. This, too, could facilitate perception of the pulse-rate mode.

do not adequately account for middle-ear transmission above this frequency), an explanation, fabricated of flimsy substance, can be suggested for the third mode. Bekesy's data suggest that the amplitude of maximal displacement of the membrane falls appreciably (about 12 db/octave or more) for frequencies above 1000 cps. In this region, then, that part of the membrane responding to the lowest-frequency component would exceed in amplitude those parts responding to higher-frequency components. If amplitude of displacement is at all important in the conversion process (and it most probably is), then the third mode is favored *provided* the lowest-frequency component is not too high in harmonic number. As indicated earlier, the third mode has been observed when either the fundamental, or the fundamental and second harmonic, is rejected from the stimulus. This mode has obtained in our pitch-matching experiments for fundamentals in the frequency range around 1000 cps and slightly higher.

One final comment is of interest along these same lines. It has been reported in the literature that if a periodic train of positive pulses is high-pass filtered at around 3000 and 4000 cps, one hears a "residue" pitch equal to the fundamental frequency. Our models suggest, however, a response more nearly correlated with pulse rate. If one uses a stimulus in which pulse rate and fundamental frequency are confounded (as with positive pulses), then the former result might obtain. If, on the other hand, a stimulus such as alternate positive and negative pulses were used, the subjective impression may well be that of pulse rate. If the latter is in fact the case, then a fundamental "residue" pitch does not exist for this condition.*

X. ACKNOWLEDGMENT

I wish to thank J. L. Perry of the Acoustics Research Department of Bell Telephone Laboratories for his capable assistance in performing many of the numerical evaluations and in plotting the results.

APPENDIX

Inverse Transforms for $F_1(s)$, $F_2(s)$ and $F_3(s)$

When the function $F_1(s)$ of (7) is disencumbered of its constants, the problem of inverse transformation amounts to calculating the inverse

* Since drafting this paper, I have set up the latter experiment and listened to alternate positive and negative pulses HP-filtered at 3000 and 4000 cps. I made pitch matches fairly consistently at the pulse rate. A second listener, on the other hand, made matches that were generally higher than the pulse rate, suggesting that my preconceived notions may have influenced my data. It is unequivocal, however, that one would not match to the fundamental frequency.

transform of:

$$K_1(s) = \left(\frac{s+\epsilon}{s+\gamma}\right)\left[\frac{1}{(s+\alpha)^2+\beta^2}\right]^2$$
$$= \left[\frac{1}{(s+\alpha)^2+\beta^2}\right]^2 + \left(\frac{\epsilon-\gamma}{s+\gamma}\right)\left[\frac{1}{(s+\alpha)^2+\beta^2}\right]^2 \quad (31)$$
$$= K_a(s) + K_b(s).$$

The inverses of $K_a(s)$ and $K_b(s)$ can be obtained in the usual manner by making partial fraction expansions in terms of the singularities, account being taken of the order of the poles, and evaluating the residues in each pole. Or, having got the inverse for $K_a(s)$, the inverse for $K_b(s)$ can be computed from:

$$K_b(t) = [(\epsilon-\gamma)e^{-\gamma t}] * [\mathfrak{L}^{-1}K_a(s)], \quad (32)$$

where $*$ indicates convolution.

For the present case these standard procedures prove rather cumbersome and messy. Because of the favorable initial values of the function and its first two derivatives [namely, $k_1(0_+) = k_1'(0_+) = k_1''(0_+) = 0$], derivative relationships can be used to obviate evaluating residues and performing the convolution.* The derivative relations of use here are the following: If the function $f(t)$ has the Laplace transform $F(s)$, then

$$(-1)^n \frac{d^nF(s)}{ds^n} = t^nf(t), \quad (33)$$

and

$$\frac{d^nf(t)}{dt^n} = s^nF(s) - s^{n-1}f(0_+) - s^{n-2}f'(0_+) - \cdots - f^{n-1}(0_+). \quad (34)$$

We start with two well-known transform pairs:

$$\frac{1}{(s+\alpha)^2+\beta^2} \rightarrow \frac{1}{\beta}e^{-\alpha t}\sin\beta t = h_1(t), \quad (35)$$

and

$$\frac{(s+\alpha)}{[(s+\alpha)^2+\beta^2]} \rightarrow e^{-\alpha t}\cos\beta t = h_2(t). \quad (36)$$

Applying (33) through (36) gives

$$\frac{[(s+\alpha)^2-\beta^2]}{[(s+\alpha)^2+\beta^2]^2} \rightarrow te^{-\alpha t}\cos\beta t = th_2(t). \quad (37)$$

* I am indebted to B. F. Logan of the Acoustics Research Department of Bell Telephone Laboratories, who pointed out to me the utility of the derivative relationships in obtaining transforms for these functions.

One notices that $K_a(s)$ can be expressed as a simple combination of (35) and (37), namely,

$$\frac{1}{[(s+\alpha)^2+\beta^2]^2} = \frac{1}{2\beta^2}\left\{\frac{1}{(s+\alpha)^2+\beta^2} - \frac{(s+\alpha)^2-\beta^2}{[(s+\alpha)^2+\beta^2]^2}\right\} \tag{38}$$

and

$$\frac{1}{[(s+\alpha)^2+\beta^2]^2} \rightarrow \frac{1}{2\beta^2}(h_1 - th_2). \tag{39}$$

Application of (34) through (39) gives

$$\frac{s}{[(s+\alpha)^2+\beta^2]^2} \rightarrow h_1\left(\frac{t}{2} - \frac{\alpha}{2\beta^2}\right) + h_2\frac{\alpha t}{2\beta^2} \tag{40}$$

and

$$\frac{s^2}{[(s+\alpha)^2+\beta^2]^2} \rightarrow h_1\left(\frac{\alpha^2+\beta^2}{2\beta^2} - \alpha t\right) + h_2\left(\frac{\beta^2-\alpha^2}{2\beta^2}t\right). \tag{41}$$

The inverse of $K_a(s)$ is, therefore, (39). The inverse of $K_b(s)$ can be obtained from a partial fraction expansion followed by application of (39), (40) and (41). Expand $K_b(s)$ as:

$$\left(\frac{\epsilon-\gamma}{s+\gamma}\right)\frac{1}{[(s+\alpha)^2+\beta^2]^2} = \frac{A}{(s+\gamma)} + \frac{G(s)}{[(s+\alpha)^2+\beta^2]^2}, \tag{42}$$

where A is a constant and

$$G(s) = (a_0 + a_1 s + a_2 s^2 + a_3 s^3).$$

If A and $G(s)$ are evaluated, one gets

$$\begin{aligned}
A &= \frac{(\epsilon-\gamma)}{[(s+\alpha)^2+\beta^2]^2}\bigg|_{s=-\gamma} = \frac{(\epsilon-\gamma)}{[\gamma^2 - 2\alpha\gamma + \alpha^2 + \beta^2]^2}, \\
a_0 &= \frac{1}{\gamma}[\epsilon - \gamma - A(\alpha^2+\beta^2)^2], \\
a_1 &= A[\gamma(4\alpha-\gamma) - 2(3\alpha^2+\beta^2)], \\
a_2 &= -A(4\alpha-\gamma), \\
a_3 &= -A.
\end{aligned} \tag{43}$$

The inverse transform of $K_b(s)$, therefore, is a summation of terms (39) through (41), with the appropriate multiplicative constants.

Two differentiations (with respect to s) of (35) give the transform pair:

$$\frac{[(s+\alpha)^2 - \beta^2/3]}{[(s+\alpha)^2 + \beta^2]^3} \rightarrow \frac{1}{6} t^2 h_1 , \tag{44}$$

which is the function used as the model $F_3(s)$ of (13).

In an essentially parallel manner, one obtains the pair:

$$\frac{s}{[(s+\alpha)^2 + \beta^2]^3} \rightarrow \frac{1}{8\beta^4} [h_1(\alpha\beta^2 t^2 + \beta^2 t - 3\alpha) + h_2(3\alpha t - \beta^2 t^2)]. \tag{45}$$

This is the function used as the model $F_2(s)$ of (11).

REFERENCES

1. Flanagan, J. L. and Guttman, N., Pitch of Periodic Pulses, J. Acoust. Soc. Am., **31,** 1959, p. 123.
2. Flanagan, J. L. and Guttman, N., Pitch of Periodic Pulses Without Fundamental Component, J. Acoust. Soc. Am., **31,** 1959, p. 836.
3. von Bekesy, G., Variations of Phase Along the Basilar Membrane with Sinusoidal Vibrations, J. Acoust. Soc. Am., **19,** 1947, p. 452.
4. von Bekesy, G., Über die Resonanzkurve und die Abklingzeit der verscheidenen Stellen der Schneckentrennwand, Akust. Zeit., **8,** 1943, p. 66; J. Acoust. Soc. Am., **21,** 1949, p. 245.
5. von Bekesy, G., Über die Schwingungen der Schneckentrennwand beim Präparat und Ohrenmodell, Akust. Zeit., **7,** 1942, p. 173; J. Acoust. Soc. Am., **21,** 1949, p. 233.
6. Zwislocki, J., Some Impedance Measurements on Normal and Pathological Ears, J. Acoust. Soc. Am., **29,** 1957, p. 1312.

Erratum

On page 747 of "The Theory and Design of Chirp Radars" in the July 1960 Bell System Technical Journal, the analytical work attributed to A. W. Schelling should correctly be credited to J. C. Schelleng.